

# Organic Guests within Zeolites: Xenon as a Photophysical Probe<sup>†</sup>

V. Ramamurthy

Contribution from Central Research and Development, Experimental Station, The DuPont Company,<sup>‡</sup> Wilmington, Delaware 19880-0328

Received October 22, 1993. Revised Manuscript Received December 10, 1993<sup>®</sup>

**Abstract:** Location and motion of aromatic guest molecules within Na X and Na Y zeolites have been probed with xenon. Xenon perturbs the photophysical properties of the excited singlet state of aromatic guest molecules through the external heavy atom effect. Naphthalene, phenanthrene, and pyrene have been used as guests, and they are nonuniformly distributed within zeolites, as indicated by their multiexponential decay of excited singlet states. Of the many locations in which the guest molecules are speculated to be present, only one has photophysical properties which are influenced by the presence of xenon. Diffusion coefficients estimated by the photophysical method presented here compare favorably with the numbers obtained by other conventional methods.

## Introduction

During the past few years xenon has been an efficient adsorbate for probing the pore structure and guest location and measuring the rates of intracrystalline self-diffusion within zeolites.<sup>1</sup> In these studies the sensitivity of the nuclear shielding of the spin  $1/2$   $^{129}\text{Xe}$  to the environment (and therefore the chemical shift of Xe in NMR spectra) is utilized.<sup>2</sup> One of the less appreciated, but well-established, properties of xenon is its heavy atom characteristics which offer an efficient spin-orbit-coupling quenching mechanism to the excited guest molecules with which it comes into contact.<sup>3</sup> This property of xenon has been utilized by us to probe the distribution and motion of molecules within zeolites. Photophysical characteristics (emission and excited-state lifetime) of zeolite-included aromatic guest molecules (pyrene, phenanthrene, and naphthalene) are perturbed, as a result of the "external heavy atom effect", by coadsorbed xenon molecules. Information concerning distribution (nonhomogeneous)<sup>4</sup> and location of guest molecules within zeolites comes from a remarkable feature observed in the quenching process, "selectivity". Diffusion of molecules on surfaces of zeolites is measured via conventional adsorption techniques or through modern NMR techniques.<sup>5</sup> The experimentally simple photophysical quenching technique which has been utilized in this study

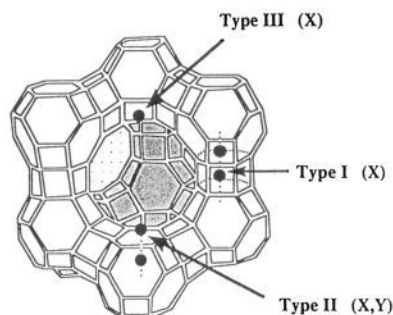


**Figure 1.** Structure of the supercages of X and Y zeolites. Cation positions are shown as Types I, II, and III.

to monitor the diffusion of guest molecules has not been widely recognized thus far in the area of zeolite chemistry.<sup>6</sup>

Zeolites may be regarded as open structures of silica in which aluminum has been substituted in a fraction of the tetrahedral sites.<sup>7</sup> The frameworks thus obtained contain pores, channels, and cages. The topological structure of X- and Y-type zeolites (also known as faujasites) consists of an interconnected three dimensional network of relatively large spherical cavities termed supercages (diameter of about 13 Å; Figure 1). Each supercage is connected tetrahedrally to four other supercages through 8-Å windows or pores. The interior of zeolites X and Y also contains, in addition to supercages, smaller sodalite cages. The windows to the sodalite cages are too small to allow organic molecules access. Charge-compensating cations present in the internal structure are known to occupy three different positions (Figure 1) in the zeolites X and Y. The above description of the cation location should be considered as a simplified model, since the exact location depends on a number of factors such as the presence of adsorbent molecules, temperature, framework composition, and the size and charge of the cations. Only cations present within the supercages are expected to be readily accessible to the adsorbed organic molecule.

<sup>†</sup> Dedicated to Professor J. K. Thomas on the occasion of his 60th birthday.

<sup>‡</sup> Contribution No. 6733.

<sup>®</sup> Abstract published in *Advance ACS Abstracts*, February 1, 1994.

(1) (a) Chen, Q. J.; Fraissard, J. *J. Phys. Chem.* **1992**, *96*, 1814. (b) Ryoo, R.; Cho, S. J.; Pak, C.; Kim, J. G.; Ihm, S. K.; Lee, J. Y. *J. Am. Chem. Soc.* **1992**, *114*, 76. (c) Liu, S. B.; Ma, L. J.; Lin, M. W.; Wu, J. F.; Chen, T. L. *J. Phys. Chem.* **1992**, *96*, 8120. (d) Heink, W.; Karger, J.; Pleifer, H.; Stallmach, F. *J. Am. Chem. Soc.* **1990**, *112*, 2175. (e) Karger, J.; Pleifer, H.; Stallmach, F.; Spindler, H. *Zeolites* **1990**, *10*, 288. (f) de Menorval, L. C.; Raftery, D.; Liu, S. B.; Takegoshi, K.; Ryoo, R.; Pines, A. *J. Phys. Chem.* **1990**, *94*, 27. (g) Ripmeester, J. A.; Ratcliffe, C. I. *J. Phys. Chem.* **1990**, *94*, 7652. (h) Ryoo, R.; Liu, S. B.; de Menorval, L. C.; Takegoshi, K.; Chmelka, B.; Trecocke, M.; Pines, A. *J. Phys. Chem.* **1987**, *91*, 6575.

(2) (a) Ito, T.; Fraissard, J. *J. Chem. Phys.* **1982**, *76*, 5225. (b) Ripmeester, J. A. *J. Am. Chem. Soc.* **1982**, *104*, 289.

(3) (a) Robinson, G. W. *J. Mol. Spectrosc.* **1961**, *6*, 58. (b) Horrocks, A. R.; Kearvell, A.; Tickle, K. Wilkinson, F. *Trans. Faraday Soc.* **1966**, *62*, 3393. (c) Horrocks, A. R.; Wilkinson, F. *Proc. R. Soc. London. A* **1968**, *306*, 257. (d) Carroll, F. A.; Quina, F. H. *J. Am. Chem. Soc.* **1976**, *98*, 1. (e) Scully, F.; Nylund, T.; Palensky, F.; Morrison, H. *J. Am. Chem. Soc.* **1978**, *100*, 7352. (f) Morrison, H.; Miller, A. *Tetrahedron* **1981**, *37*, 3405. (g) Morgan, M. A.; Pimental, G. C. *J. Phys. Chem.* **1989**, *93*, 3056.

(4) (a) Weiss, R. G.; Ramamurthy, V.; Hammond, G. S. *Acc. Chem. Res.* **1993**, *26*, 530. (b) Ramamurthy, V.; Weiss, R. G.; Hammond, G. S. *Adv. Photochem.* **1993**, *18*, 67.

(5) Karger, J.; Ruthven, D. M. *Diffusion in Zeolites*; John Wiley & Sons: New York, 1992.

(6) For studies on silica surfaces: (a) Drake, J. M.; Levitz, P.; Turro, N. J.; Nitsche, K. S.; Cassidy, K. F. *J. Phys. Chem.* **1988**, *92*, 4680. (b) Turro, N. J.; Zimmt, M. B.; Gould, I. R. *J. Am. Chem. Soc.* **1985**, *107*, 5826. (c) Oelkrug, D.; Uhl, S.; Wilkinson, F.; Willscher, C. J. *J. Phys. Chem.* **1989**, *93*, 4551. (d) de Mayo, P. *Pure Appl. Chem.* **1982**, *54*, 1623.

(7) (a) Breck, D. W. *Zeolite Molecular Sieves*; Krieger Publishing Company: Malabar, FL, 1984. (b) Dyer, A. *An Introduction to Zeolite Molecular Sieves*; John Wiley and Sons: Bath, U.K., 1988. (c) van Bekkum, H.; Flanigen, E. M.; Jansen, J. C., Eds. *Introduction to Zeolite Science and Practice*; Elsevier: Amsterdam, The Netherlands, 1991. (d) Szostak, R. *Molecular Sieves. Principles of Synthesis and Identification*; Van Nostrand: New York, 1989.

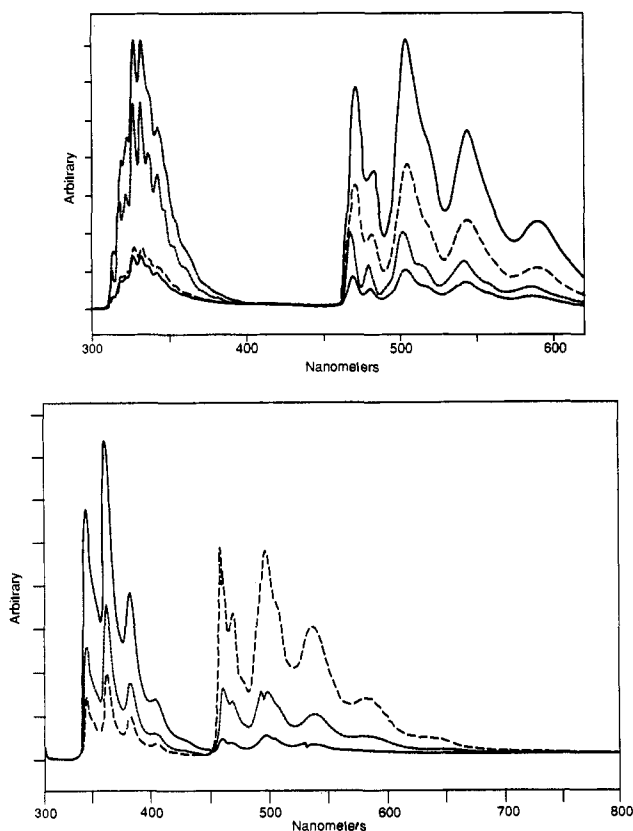


**Figure 2.** Emission spectra of naphthalene and phenanthrene in Na X at 77 K under various pressures of xenon; both at a  $\langle S \rangle$  of 0.01. (a) Naphthalene:  $\cdots$ , 0 Torr;  $\cdots$ , 18 Torr;  $-\cdot-, 100 Torr;  $-$ , 200 Torr of xenon. (b) Phenanthrene:  $-$ , 0 Torr;  $\cdots$ , 25 Torr;  $-\cdot-, 100 Torr of xenon. In both cases the emission in the region 300–400 nm corresponds to fluorescence and that in the region 450–600 nm to phosphorescence.$$

## Results

Steady-state and time-resolved emission characteristics of pyrene, naphthalene, and phenanthrene adsorbed within zeolites Na X and Na Y have been investigated. Emphasis is on the perturbation of the above characteristics by the gaseous quencher xenon. Complexes of the above aromatics with Na X and Na Y were prepared by the method outlined in the Experimental Section. The loading level ( $\langle S \rangle$ : number of molecules per supercage) of the aromatics was maintained in the range 0.005–0.05. This corresponded to an average local concentration of 0.01–0.1 M.<sup>8</sup> Hexane washings of the complex reduce the amount of aromatics adsorbed on the external surfaces of zeolites. At room temperature, steady-state emission spectra of the aromatics included within zeolites consisted of intense fluorescence and fairly weak phosphorescence. The emission characteristics of all three aromatics were influenced by the quencher xenon; at room temperature fluorescence intensity decreased with the increase in the pressure of xenon. As illustrated in Figure 2 with phenanthrene and naphthalene the fluorescence quenching at 77 K was accompanied by an increase in the intensity of phosphorescence emission with the pressure of xenon. The relationship

(8) Occupancy number refers to the number of molecules per supercage. Assuming the X and Y supercage volume to be  $800 \text{ \AA}^3$ , one can convert the occupancy number to a concentration unit.<sup>9</sup> An occupancy of one atom or molecule per supercage ( $800 \text{ \AA}^3$ ) corresponds to an average local concentration of 2.08 M. Knowing this conversion factor, any occupancy number can be converted to concentration units (M). The concentration represented here is only approximate and realistically may not be comparable with solution concentration. Looking at the loading levels in this term provides a better feeling for the amount of guest within a certain volume. In this calculation volume refers to the space accessible to the guest, which may vary depending on the size of the guest.

(9) Ramamurthy, V. In *Photochemistry in Organized and Constrained Media*; Ramamurthy, V., Ed.; VCH Publishers: New York, 1991; Chapter 10, p 435.

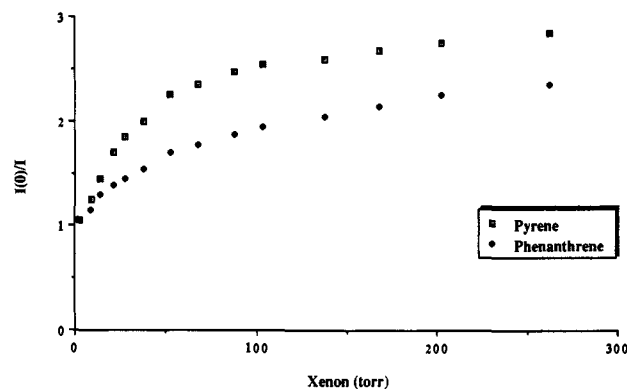


**Figure 3.** Illustrative examples of Stern–Volmer plots for the quenching of pyrene ( $\langle S \rangle$ : 0.01) and phenanthrene ( $\langle S \rangle$ : 0.01) included within Na Y by xenon. The x-axis xenon pressure does not correspond to the amount of xenon adsorbed; it only represents the pressure applied. The amount of xenon adsorbed was estimated utilizing an adsorption isotherm.

between the intensity of fluorescence ( $I_0/I$ ) and xenon pressure (Stern–Volmer plots) is shown in Figure 3 at one loading level of aromatics within Na Y. Similar plots were obtained at other loading levels of aromatics and within Na X. While a linear relationship is observed at low pressures ( $<50$  Torr), nonlinear behavior is common at higher pressures. The linear region ( $<50$  Torr) was utilized to calculate the Stern–Volmer slopes. Non-linearity at higher pressures of xenon may be the result of any, a combination, or all of the following factors: (a) variation in the diffusion coefficient of xenon with the increased loading level of xenon; (b) nonlinear dependence between adsorbed xenon and the external pressure; and (c) differences in rates of quenching of aromatics present at different sites. Two of the above features have been documented in the literature.<sup>1b,c,d,10,11</sup>

In order to calculate the quenching constants, the lifetime of the excited singlet state being quenched is required. Decay of the excited singlet state was multiexponential; however, reasonable fits with either two or three exponentials were obtained. However, we limited our analysis to two exponentials. Representative examples of lifetime data (analyzed on the basis of two exponentials) for the three aromatics at a single loading level under various pressures of xenon within Na X and Na Y are presented in Table 1. It is remarkable to note that of the two lifetimes only one is significantly influenced by xenon. As seen in Table 1, similar selectivity was also observed at 77 K independent of the fact that xenon exists as a solid at 77 K within zeolites.<sup>12</sup> Examination of Figure 4 illustrates this clearly; only the early component in the excited singlet state decay of pyrene (in Na Y) is subjected to influence by xenon. Similar to the case of the Stern–Volmer plots in Figure 3, the lifetime quenching also showed nonlinear behavior at pressures higher than 50 Torr. Quenching constants calculated from steady state spectra and time-resolved decays are summarized in Table 2. In the case of emission, total fluorescence intensity was used to calculate  $k_q$  whereas, in the case of lifetime, only the quenchable component was used. In spite of this, the agreement between the two sets of numbers is noteworthy. It is to be noted that  $k_q$  presented in the table corresponds to the sites which are quenched more readily, since only the linear region has been utilized in the estimation of rates. The concentration of xenon was converted from torr to number of molecules adsorbed per supercage utilizing adsorption isotherms available in the literature.<sup>1b,c,10</sup> The number of molecules adsorbed per supercage was converted to regular

(10) Watermann, J.; Boddenberg, B. *Zeolites* 1993, 13, 427.

(11) (a) Pfeifer, H.; Karger, J.; Germanus, A.; Schirmer, W.; Bulow, M.; Caro, J. *Adsorpt. Sci. Technol.* 1985, 2, 229. (b) Santikary, P.; Yashonath, S.; Ananthakrishna, G. *J. Phys. Chem.* 1992, 96, 10469.

(12) (a) Cheung, T. T. P. *J. Phys. Chem.* 1992, 96, 5505. (b) Cheung, T. T. P. *J. Phys. Chem.* 1989, 93, 7549. (c) Cheung, T. T. P.; Fu, C. M.; Wharry, S. *J. Phys. Chem.* 1988, 92, 5170.

**Table 1.** Excited Singlet State Lifetimes (in ns) of Aromatics Included within Na X and Na Y<sup>a,b,c</sup>

xenon pressure (Torr; $\pm 2$ )	phenanthrene ((S):0.01)			naphthalene ((S):0.01)		pyrene ((S):0.001)	
	Na X at RT	Na X at 77 K	Na Y at RT	Na X at RT	Na X at 77 K	Na X at RT	Na Y at RT
0	34.2, 19.7	34.5, 10.7	32.8, 7.1	29.6, 14.2	67.8, 33.0	156, 68.5	116, 46.0
25	33.5, 16.3	32.4, 8.4	32.1, 5.3	31.6, 13.0	64.0, 20.0	151, 61.3	110, 27.8
50	32.9, 12.2	33.0, 5.6	32.8, 4.4	32.8, 9.9	63.3, 14.2	147, 49.8	123, 22.1
175	32.7, 9.2	33.1, 4.5	34.1, 3.7	30.7, 6.1	61.2, 12.8	144, 34.8	123, 13.4
350	31.5, 5.4	33.3, 3.4	34.1, 3.1	31.4, 5.3	61.9, 7.7	140, 26.6	120, 3.4

<sup>a</sup> Only 95% of the singlet decay can be fitted to a double-exponential decay. Approximately the initial 10–15 channels could not be included in the analysis. <sup>b</sup> To obtain the quenching constants, the lifetimes were measured at five points between 0 and 100 Torr of xenon. <sup>c</sup> All lifetimes are subject to an error of  $\pm 10\%$ .

**Table 2.** Quenching of Aromatics Included within Na X and Na Y by Xenon and Oxygen: Estimation of Rates of Quenching<sup>a</sup>

probe	occupancy level (no. of molecules/supercage)	Na X		Na Y	
		$k_q$ (emission) <sup>b</sup>	$k_q$ (lifetime) <sup>c</sup>	$10^{-5}k_q$ (emission) <sup>b</sup>	$10^{-5}k_q$ (lifetime) <sup>c</sup>
(a) Xenon					
naphthalene	0.01	$9 \times 10^5$	$6 \times 10^5$	15	
	0.1	$14 \times 10^5$	$8 \times 10^5$	21	
phenanthrene	0.01	$6 \times 10^5$	$2 \times 10^5$	18	28
	0.1	$10 \times 10^5$	$4 \times 10^5$	23	18
pyrene	0.001	$8 \times 10^4$	$6 \times 10^4$	8	5
	0.01	$5 \times 10^4$	$7 \times 10^4$	6	7
(b) Oxygen					
naphthalene	0.01	$4 \times 10^5$			
phenanthrene	0.01	$7 \times 10^5$		19	
pyrene	0.001	$5 \times 10^4$		8	

<sup>a</sup> All rates are expressed in terms of Torr<sup>-1</sup> s<sup>-1</sup>. The pressure refers to applied pressure, and the amount of xenon adsorbed is estimated on the basis of adsorption isotherms available in the literature. These numbers can be converted to number of molecules per supercage per second by using the conversion factor that 1 Torr is 0.004 molecules/supercage (in the case of Na Y) and 0.006 molecules/supercage (in the case of Na X). Similar conversion to M<sup>-1</sup> s<sup>-1</sup> is achieved by utilizing the conversion factor 1 Torr is 0.008 M (Na Y) and 0.012 M (Na X). <sup>b</sup> Numbers (in Torr<sup>-1</sup> s<sup>-1</sup>) obtained from Stern–Volmer plots of quenching of the fluorescence emission (slope =  $k_q\tau$ ). <sup>c</sup> Numbers (in Torr<sup>-1</sup> s<sup>-1</sup>) obtained through plots ( $\tau^{-1}$  vs [Xe]) of the lifetime quenching (slope =  $k_q$ ).

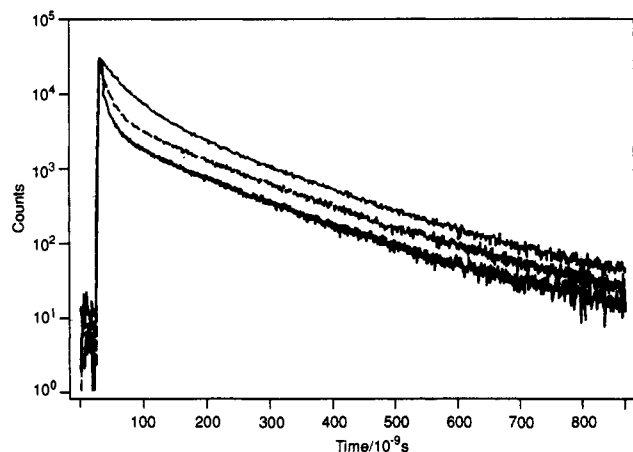


**Figure 4.** Illustrative example of the excited singlet state decay of pyrene monomer included within Na X followed by its emission (SPC data) under various pressures of xenon. Top to bottom: 0, 120, and 400 Torr of xenon.

concentration units (M) following the conversion factor that one molecule per supercage corresponds to 2.08 M.<sup>8</sup> These unit conversions are approximate, and any extension should be done with caution.

The above lifetime data suggested that, of the two locations in which aromatic molecules are present, only one is more readily accessible to xenon. This prompted us to investigate the interaction between xenon and pyrene under conditions where excimer formation occurs. Quenching of pyrene monomer and excimer emissions and lifetimes at higher loadings of pyrene ( $\langle S \rangle$ : 0.1) within Na X and Na Y with respect to the pressure of xenon was monitored. Surprisingly the excimer emission was quenched inefficiently relative to the monomer emission at low pressures of xenon (Figure 5). However, at pressures higher than 50 Torr, intensities of both monomer and excimer emissions were quenched, although at different rates. In addition, unlike

the case at low loading levels, xenon quenching showed poor selectivity in quenching of the excited state of the monomer present at two locations (Table 3).

In order to compare the quenching rates by xenon with that by a more efficient quencher, the emission intensities and lifetimes of the above three aromatics included within Na Y were monitored in the presence of various pressures of oxygen. Trends in results were broadly similar to that observed with xenon (Table 4). Quenching rates are presented in Table 2.

The mobility of xenon was fully inhibited, and the quenching was absent when the aromatics were coincubed with water within zeolites X and Y. This observation leads to two conclusions: (a) aromatic molecules are present only to a very minor extent, if at all, on the external surfaces of zeolites (had the molecules been on the surface a certain amount of quenching would be expected), and (b) xenon does not enter zeolites when the entrances and cages are blocked by water molecules.

## Discussion

**Fluorescence Quenching by Xenon.** Excited singlet state quenching by xenon, an external heavy atom perturber, is a well-known phenomenon.<sup>3</sup> At room temperature, coadsorbed xenon influences the singlet lifetime and the fluorescence emission intensity of naphthalene, phenanthrene, and pyrene included within Na X and Na Y. Although no new emissions were seen at room temperature, at 77 K the decrease in fluorescence lifetime and emission intensity was accompanied by an enhancement in the phosphorescence emission (Figure 2). Qualitative measurements of the phosphorescence decay indicated a decrease in triplet lifetime at 77 K with the increased xenon pressure. These observations are consistent with xenon acting as an external heavy atom quencher.<sup>3a</sup> The quenching mechanism must be the same both at room and low temperatures, since a similar trend in the decrease of singlet lifetime and fluorescence intensity with xenon pressure was noticed at both temperatures (Table 1).

The above effect was found to be general, as a number of other aromatics such as chrysene, acenaphthene, anthracene, and

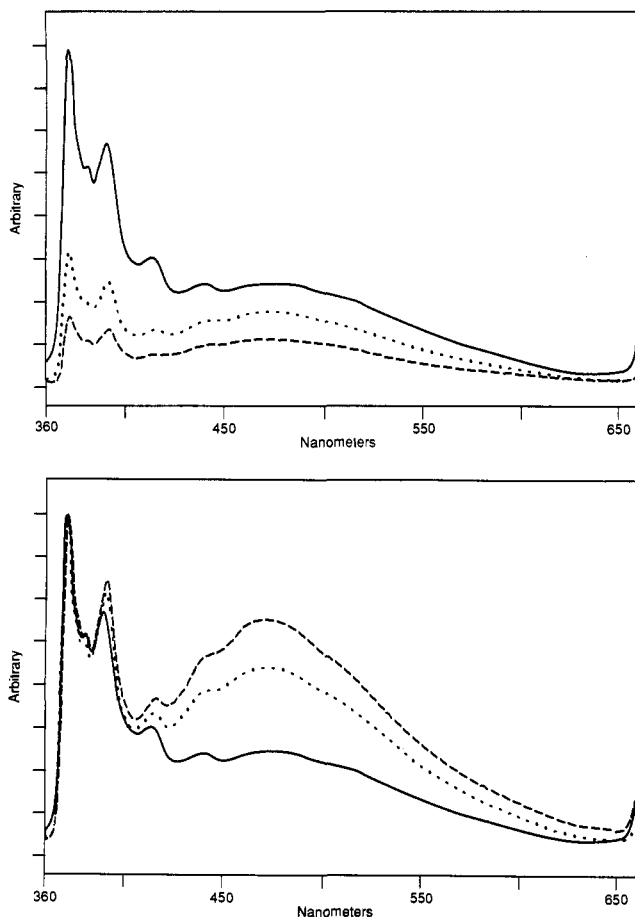


**Figure 5.** Emission spectra under various pressures of xenon at room temperature of pyrene ( $\langle S \rangle$ : 0.1) included within Na Y. Emission in the region 360–420 nm corresponds to that from monomer and that in the region  $\sim$ 420–630 to excimer: (a) spectra as recorded and (b) spectra normalized at the monomer emission to show that monomer and excimer emissions are quenched at different rates. In both cases: —, 0 Torr; ---, 11 Torr; ···, 40 Torr.

**Table 3.** Effect of Xenon on Monomer and Excimer Lifetimes (in ns) of Pyrene ( $\langle S \rangle$ :0.1) Included within Na X<sup>a,b</sup>

xenon pressure (Torr)	monomer	excimer
0	167, 56	112, 54
20	142, 47	110, 52
35	128, 40	108, 51
55	112, 32	93, 34
100	85, 24	75, 26
200	72, 19	70, 20

<sup>a</sup> Only 95% of the singlet decay can be fitted to a double-exponential decay. Approximately the initial 10–15 channels could not be included in the analysis. <sup>b</sup> All lifetimes are subject to an error of  $\pm 10\%$ .

hexahydropyrene included in Na X and Na Y and naphthalene and phenanthrene included in a number of Na<sup>+</sup>-exchanged zeolites such as M-5, ZSM-5, ZSM-11,  $\beta$ , and  $\Omega$ -5 showed intense phosphorescence at 77 K in the presence of coadsorbed xenon. However, the influence by xenon is not as powerful as that by the heavy cation Tl<sup>+</sup>. Phosphorescence emission even from olefins was recorded when they were included within Tl<sup>+</sup> X and Tl<sup>+</sup> Y.<sup>13</sup> However, with coadsorbed xenon we were unable to observe phosphorescence from any olefins. This is consistent with the known magnitude of spin-orbit coupling of xenon, which is close to that of Cs<sup>+</sup> and iodine.<sup>3a</sup>

**Selectivity in Quenching by Xenon.** Unlike the case in homogeneous solution media, fluorescence decay of pyrene, naphthalene, and phenanthrene adsorbed onto Na X and Na Y

(13) Ramamurthy, V.; Caspar, J. V.; Eaton, D. F.; Kuo, E. W.; Corbin, D. R. *J. Am. Chem. Soc.* **1992**, *114*, 3882.

**Table 4.** Excited Singlet State Lifetimes (in ns) of Aromatics Included within Na X and Na Y: Effect of Oxygen<sup>a,b</sup>

oxygen pressure (Torr; $\pm 5$ )	phenanthrene ( $\langle S \rangle$ :0.01)		naphthalene ( $\langle S \rangle$ :0.01)		pyrene ( $\langle S \rangle$ :0.01)	
	Na X at RT	Na Y at RT	Na X at RT	Na X at RT	Na Y at RT	
0	34.2, 19.7	32.8, 9.8	29.6, 14.2	156, 68.5	116, 46.0	
25	32.5, 14.8	32.1, 7.1	32.4, 12.3	161, 54.3	116, 34.6	
50	33.6, 11.6	32.8, 5.1	32.8, 9.9	157, 45.4	126, 22.1	
175	34.0, 6.3	33.3, 4.5	30.7, 6.1	148, 41.4	126, 13.5	
350	33.9, 5.0	29.3, 3.3	31.4, 5.3	141, 33.1		

<sup>a</sup> Only 95% of the singlet decay can be fitted to a double-exponential decay. Approximately the initial 10–15 channels could not be included in the analysis. <sup>b</sup> All lifetimes are subject to an error of  $\pm 10\%$ .

does not follow single-exponential decay (Table 1). More than 95% of the fluorescence decay can be satisfactorily analyzed on the basis of two exponential decay, indicating that there are primarily two families of sites in which these aromatic molecules are located. A third minor component with a very short lifetime ( $\sim$ 1–3 ns) is revealed when the analysis is carried out by a three-exponential function. Much of the short component could either result from scattering of the excitation beam by solid samples or be due to a static quenching process. Because of this complication the analysis and discussion are restricted to two exponentials. Indeed when the analysis of the decay was carried out on the basis of a distribution function, a bimodal distribution was observed.<sup>14</sup> The above two-site model is consistent with previous <sup>2</sup>H NMR studies on phenanthrene in various cation-exchanged X zeolites.<sup>15</sup> It was inferred from <sup>2</sup>H NMR studies that phenanthrene molecules are located at two different sites within X zeolites and that the extent of occupation of these sites is temperature dependent. Further, one of these sites is suggested to be close to the cation—ion bound. As expected, on a nanosecond time scale such a distribution is maintained. Photophysical studies carried out here provide information concerning the environments around the guest molecules at these two sites. It has been established that the lifetime of the pyrene excited singlet state is related to the polarity of the medium; the lifetime is fairly long in a nonpolar medium (e.g., cyclohexane: 430 ns) and is relatively short in a polar medium (e.g., dimethylformamide: 280 ns).<sup>16</sup> On the basis of the relationship between lifetime and polarity of the medium, it is likely that the one with the shorter lifetime corresponds to the pyrene molecule closer to the cation (higher electric field/micropolarity) and the one with the longer lifetime refers to the pyrene farther from the cation (lower electric field/micropolarity).<sup>17</sup> This conclusion is supported by the time-resolved emission spectra displayed in Figure 6. Vibrational features in the emission spectra of pyrene included in Na Y are found to be time dependent in the time range 1–900 ns. The intensity of the first band at 373 nm is fairly strong at early times and is weak at later times. It has been established in homogeneous solution that the intensity of this band is dependent on the polarity of the medium.<sup>18</sup> The intensity variation observed above is consistent with the proposal that pyrene molecules are present

(14) Complete decay of excited singlet states of these systems has been analyzed on the basis of a distribution function based on the Fredholm integral, and this has been discussed in previous publications: (a) Ramamurthy, V.; Sanderson, D. R.; Eaton, D. F. *J. Phys. Chem.*, in press. (b) Ramamurthy, V. *Mol. Cryst. Liq. Cryst.*, in press. For the purpose of this paper, analysis based on two exponentials was felt adequate.

(15) Hepp, M. A.; Ramamurthy, V.; Corbin, D. R.; Dybowski, C. *J. Phys. Chem.* **1992**, *96*, 2629.

(16) (a) Nakajima, A. *Bull. Chem. Soc. Jpn.* **1973**, *46*, 2602. (b) Hara, K.; Ware, W. R. *Chem. Phys.* **1980**, *51*, 61.

(17) (a) Ramamurthy, V.; Sanderson, D. R.; Eaton, D. F. *Photochem. Photobiol.* **1992**, *56*, 297. (b) Ramamurthy, V.; Caspar, J. V. *Mol. Cryst. Liq. Cryst.* **1992**, *211*, 211. (c) Ramamurthy, V.; Eaton, D. F. In *Proceedings of the 9th International Zeolite Conference*; von Ballmoos et al., Eds.; Butterworth-Heinemann: New York, 1993; pp 587–594.

(18) (a) Nakajima, A. *Bull. Chem. Soc. Jpn.* **1971**, *44*, 3272. (b) Kalyanasundaram, K.; Thomas, J. K. *J. Am. Chem. Soc.* **1977**, *99*, 2039. (c) Dong, D. C.; Winnik, M. A. *Photochem. Photobiol.* **1982**, *35*, 17.

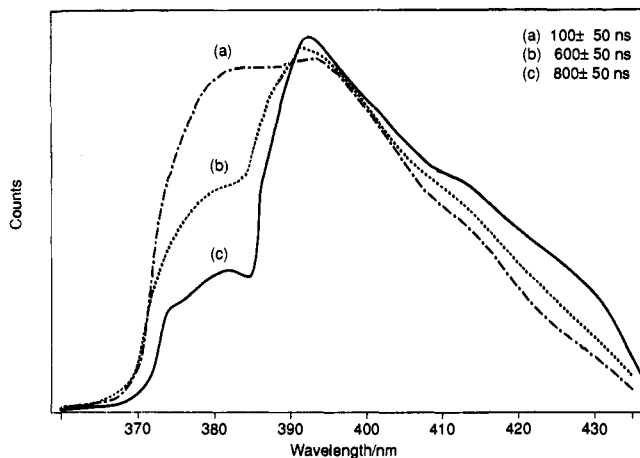


**Figure 6.** Time-resolved emission spectra of pyrene monomer included within dry Na Y. The intensity of the first band depends on the time window.

under two different microenvironments, one highly polar and the other moderately polar. Although the  $^2\text{H}$  NMR and the above photophysical studies suggest that one of the sites in which the aromatic molecule is located is cationic (ion bound), no conclusive information concerning the location of the other is forthcoming.

The remarkable selectivity observed in the quenching of naphthalene, phenanthrene, and pyrene included within Na Y and Na X, we believe, throws light on the location of the second site. Perusal of Table 1 and Figure 4 clearly indicates that of the two lifetimes only the shorter one is considerably influenced by xenon. We interpret this to mean that the site at which favorable interaction (for the heavy-atom effect to operate) occurs between the aromatic molecules and xenon is the cationic site. Neutron diffraction experiments carried out with benzene as the adsorbate within Na Y and Na X suggest that, in addition to benzene molecules being present at the cationic site, they are also adsorbed (parallel) at windows connecting two supercages.<sup>19</sup> At the 12-ring window site, the interaction occurs through van der Waals forces and via acid-base interactions between the C-H bonds of benzene and the oxygens of the 12-ring window. While benzene may fit, the aromatic molecules investigated here are too large to fit in a parallel geometry at the window sites. Even if they are adsorbed in this fashion at the window, reasons for absence of quenching by xenon are not clear, since access to these sites by xenon is not restricted (each supercage is endowed with four windows) and the  $\pi$ -cloud will still be exposed to xenon for interaction. Supercages of X and Y zeolites are fairly open, and one cannot visualize any other positions within the supercage where these large molecules will be stabilized through adsorption. The above selective quenching, we believe, can be understood on the basis that aromatic molecules are located at the windows connecting two cages (similar to benzene but not in the same geometry) such that their long axis is parallel to the axis connecting two supercages. In this geometry the  $\pi$ -cloud of the aromatic framework, facing and interacting with the walls of the window, will not be accessible to xenon. Although xenon can access these sites through other entrances to the supercage, a favorable geometry for spin-orbit coupling may not be achievable.<sup>20</sup> In the case of pyrene within Na X, at higher loading levels, both lifetimes were influenced by xenon (Table 3), suggesting that pyrene molecules present at windows connecting two cages are displaced slightly into one of the cages so that xenon can interact with the

$\pi$ -cloud. This may be a result of the larger size of pyrene compared to naphthalene and phenanthrene and due to the presence of higher crowding (lesser free volume) in X than in Y zeolites due to the larger number of cations in the former.

The above selectivity in quenching might also result if xenon prefers to adsorb on only one of the two sites in which the aromatic molecules are present. However, the lack of quenching of aromatic guest molecules present at one of the many sites clearly argues for the nonuniform distribution of guests within zeolites. NMR studies by a number of workers point out that xenon prefers to adsorb at a number of different sites within faujasites.<sup>21</sup> While at low temperatures ( $< -80^\circ\text{C}$ ) xenon is fixed in a potential well, at room temperature, xenon is shown to exchange rapidly between these sites. Further, while in silver-exchanged X and Y zeolites there is a clear preference for the cationic sites over the others, in Na-exchanged zeolites no such preference was evident.<sup>22</sup>

It has been established earlier that pyrene included within Na X and Na Y at higher loadings ( $\langle S \rangle$  over 0.05) gives rise to both monomer and excimer emissions.<sup>17,23</sup> Evidences in favor of the former being from preaggregates have already been presented. Results on xenon quenching at low pressures further support the original suggestion concerning the origin of excimer within the supercages—excimers are formed from preaggregates (static excimers) and not from free monomers (dynamic excimer). In Figure 5, the emission spectra of pyrene included within Na Y and Na X at various pressures of xenon are presented. It is clear from Figure 5a that, at pressures lower than 50 Torr of xenon, the intensity of excimer emission is not decreased to the same extent as that of the monomer. This is brought out more vividly in Figure 5b, where monomer emission intensities have been normalized to highlight the changes. Relatively slow quenching of excimer by xenon may be the result of either the pyrene present as preaggregates being too short lived in the excited state for xenon to interact or the cages containing preaggregates being too crowded for xenon to enter. A point to note is that, at higher pressures, excimer emission and lifetime are quenched by xenon (Table 3). Thus, it is evident that quenching by xenon is very selective: of the three locations in which aromatic molecules are present (cationic, window, and preaggregates) within the supercages, only one (cationic site) is readily accessible to xenon.

Observations made here are not without precedent although all the earlier studies have utilized oxygen as the quencher. Evidence in favor of an inhomogeneous distribution of aromatic ketones within silicalite (with a structure analogous to that of ZSM-5) has been provided by Casal and Scaiano through oxygen quenching of the ketone triplets.<sup>24</sup> Their conclusions bear close similarity to ours although their observations pertain to a different zeolite; triplets with two lifetimes being quenched at different rates by oxygen were identified. Thomas and co-workers have shown that pyrene included within Na X and Na Y can be quenched by oxygen.<sup>23</sup> Their analyses of excited monomer decay (followed by transient absorption during laser flash photolysis experiments) was based on a single exponential and thus was unable to provide information concerning the selectivity in oxygen quenching of the excited singlet state of the monomer. However, they observed and acknowledged the decays to be multi exponential and, further, showed that monomer and excimer states were quenched at slightly different rates by oxygen. Turro and co-workers have established that photolysis of dibenzyl ketone included within Na X proceeds through three stages, and this gives rise to primary, secondary, and free radicals. They were

(19) (a) Fitch, A. N.; Jobic, H.; Renouprez, A. *J. Chem. Soc., Chem. Commun.* **1985**, 284. (b) Fitch, A. N.; Jobic, H.; Renouprez, A. *J. Phys. Chem.*, **1986**, *90*, 1311. (c) Czjek, M.; Vogt, T.; Fuess, H. *Angew. Chem., Int. Ed. Engl.* **1989**, *28*, 770.

(20) (a) Weinzierl, G.; Friedrich, J. *Chem. Phys. Lett.* **1981**, *80*, 55. (b) Ramamurthy, V.; Caspar, J. V.; Corbin, D. R.; Schlyer, B. D.; Maki, A. H. *J. Phys. Chem.* **1990**, *94*, 3391.

(21) (a) Chen, Q. J.; Fraissard, J. *J. Phys. Chem.* **1992**, *96*, 1809. (b) Smith, M. L.; Dybowski, C. *J. Phys. Chem.* **1991**, *95*, 4942. (c) Cheung, T. T. P.; Fu, C. M. *J. Phys. Chem.* **1989**, *93*, 3740.

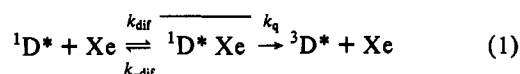
(22) (a) Grosse, R.; Gedeon, A.; Watermann, J.; Fraissard, J.; Boddenberg, B. *Zeolites* **1992**, *12*, 909. (b) Watermann, J.; Boddenberg, B. *Zeolites* **1993**, *13*, 427.

(23) Liu, X.; Iu, K. K.; Thomas, J. K. *J. Phys. Chem.* **1989**, *93*, 4120.

(24) Casal, H. L.; Scaiano, J. C. *Can. J. Chem.* **1985**, *63*, 1308.

able to quench selectively these three types of radicals by controlling the pressure of oxygen.<sup>25</sup>

**Interpretation of the Observed Quenching Constant.** Equation 1 illustrates the kinetic sequence of the xenon-quenching process.



$$k_{\text{obs}} = \frac{k_{\text{diff}}k_{\text{q}}}{k_{\text{-diff}} + k_{\text{q}}} \quad (2)$$

The observed rate of quenching (collected in Table 2) as presented in eq 2 is a combination of the rate of actual quenching and the rate of diffusion. Under the conditions where the rate of quenching is much faster than the rate of diffusion, the observed quenching rate is in fact the rate of diffusion. When the quenching rate is comparable or slower than the rate of diffusion, the observed rate of quenching is smaller than the rate of diffusion.

Observed rates of quenching are expected to follow the trend that has been reported in solution if the actual quenching process rather than diffusion is controlling (limiting) the quenching phenomenon. In ethanol solution the rates of quenching of excited singlets of naphthalene, phenanthrene, and pyrene by xenon are reported to be  $1.1 \times 10^9$ ,  $0.29 \times 10^9$ , and  $0.022 \times 10^9 \text{ M}^{-1} \text{ s}^{-1}$ , respectively.<sup>3b,26</sup> Examination of Table 2 reveals no such trend. Excited-state quenching of pyrene by xenon within zeolites is slow, but we believe that it is due to steric reasons. Therefore, the numbers measured in this study, we believe, reflect the rate of diffusion of quencher and/or quenchee within zeolites. This conclusion is supported by the observations made with oxygen as the quencher. Oxygen was chosen as the quencher, since its diffusion coefficient within zeolites is reported to be close to that of xenon<sup>27</sup> and it is known to quench the excited singlet states of aromatics in solution by a diffusion-limited energy transfer process ( $\sim 10^{10} \text{ M}^{-1} \text{ s}^{-1}$ ).<sup>28</sup> We thought that the quenching rates measured for oxygen should be close to those measured for xenon if indeed diffusion limits the quenching process in these two cases. Indeed the measured rates of quenching of the excited singlets of naphthalene, phenanthrene, and pyrene within Na X and Na Y by oxygen are very close to the numbers measured for quenching by xenon (Table 2).

While the above studies point out that the quenching rates measured are a reflection of molecular movements on the surfaces of zeolites, they do not indicate which one of the two (or both)—quencher and/or quenchee—is moving. Diffusion coefficients of a number of molecules within X and Y zeolites have been measured by a variety of techniques, although the numbers for the same compound from two techniques rarely agree. More reliable numbers are generally obtained through the pulsed field gradient NMR (PFG NMR) technique. Diffusion coefficients (at  $\sim 400 \text{ K}$ ) obtained through PFG NMR for xenon, benzene, and xylenes are  $1.5 \times 10^{-9}$ ,  $2 \times 10^{-11}$  and  $5 \times 10^{-11} \text{ m}^2 \text{ s}^{-1}$  respectively.<sup>29</sup> The molecules investigated here—pyrene, naphthalene, and phenanthrene—are expected to have diffusion coefficients much smaller than benzene and xylenes. Indeed the diffusion coefficient for dimethylnaphthalene has been reported to be  $\sim 10^{-16} \text{ m}^2 \text{ s}^{-1}$  (gravimetric technique).<sup>29</sup> Large differences in diffusion coefficients between the aromatic and xenon suggest

that within the lifetime of the excited state ( $\sim 40 \text{ ns}$ ) xenon will move much longer distances than the aromatic molecule. The distances traveled in the time range of 40 ns by xenon and the aromatic were *qualitatively* estimated (using the Einstein-Smoluchowski equation:  $D = u^2(2t)^{-1}$  where  $D$  is diffusion coefficient and  $u$  is distance traveled in time  $t$ )<sup>30</sup> to be 110 and  $\sim 3 \text{ \AA}$ , respectively. Thus the measured quenching rates within zeolites correspond to the diffusion rate of xenon rather than that of the guest aromatic molecule.

The values of  $k_{\text{diff}}$  obtained in this study compare favorably with the one calculated on the basis of the Smoluchowski equation ( $k_{\text{diff}} = 4\pi N\sigma D$ , where  $N$  is Avagadro's number,  $\sigma$  is the reaction distance, assumed to be  $8 \text{ \AA}$ , and  $D$  is the diffusion coefficient) using the known diffusion coefficient of xenon.<sup>1d</sup> It is very important to note that the  $k_{\text{diff}}$  values estimated here are meaningful only in a qualitative sense, since the equations used to make the estimate were developed specifically for motions in an isotropic solution environment. The point we wish to emphasize is that a simple photophysical method utilized here provides diffusion parameters which are comparable to those of other methods reported in the literature. Quantitative interpretation of the measured numbers requires understanding the detailed motion of guest molecules within zeolites, a process not likely to be the same as that in isotropic solution. Two observations are worth noting: (a) diffusion of xenon within Na X is slightly smaller than that in Na Y (probably a result of the larger number of cations in X) and (b) diffusion is slower in pyrene-entrapped zeolites than in naphthalene- and phenanthrene-enclosed zeolites (probably a result of the larger size of pyrene with respect to the other two).

Thus the method to measure diffusion rates of gaseous molecules presented here is fairly simple compared to what is available in the literature. Further sophistication and improvement is needed to utilize this technique to monitor the motions of other guest molecules. Considerable interest exists in understanding diffusion of molecules within zeolites,<sup>3,31</sup> and a simple technique such as the one presented here is expected to be of great value in understanding the mechanism of diffusion of guest molecules within zeolites. A simple model needs to be generated to interpret the quenching rates measured in studies such as this. Quenching by gaseous molecules such as xenon and oxygen not only provides information concerning motion of the quencher but also yields details about the environment around guest molecules. Further work is required to understand these processes in detail.

## Experimental Section

**Materials.** LZ-Y52 (Na Y) and 13 X (Na X), in powder form, were obtained from Aldrich and used following dehydration. Pyrene, naphthalene, and phenanthrene were obtained from Aldrich or Fluka (99.9+-% purity) and were recrystallized from ethanol three times to constant melting point.

**Activation of Zeolites.** In general, ca. 250 mg of zeolite was placed in a silica crucible and heated at  $500 \text{ }^\circ\text{C}$  for about 12 h. The freshly activated zeolites were rapidly cooled in air to  $\sim 50 \text{ }^\circ\text{C}$  and added to solutions of the guests of interest. Zeolites were used immediately after activation. In general, we have found that the time required for these activated zeolites to readsorb water to their full capacity is about 2 h under our laboratory conditions, though the duration varies with the zeolite and the laboratory humidity. The rehydration is easily monitored by keeping the activated zeolites on the pan of an analytical balance and watching the weight increase.

**Preparation of Zeolite-Aromatic Complexes.** Known amounts of aromatics and the activated zeolites were stirred together in 20 mL of hexane for about 10 h. In a typical preparation, 250 mg of the zeolite and 0.01 mg of the aromatic guest were taken. White powder collected

(25) Garcia-Garibay, M. A.; Lei, X. G.; Turro, N. J. *J. Am. Chem. Soc.* 1992, 114, 2750.

(26) These quenching rates were calculated on the basis of  $\tau_0$ . The same trend was maintained when they were recalculated utilizing measured  $\tau$  (Murov, S. *Handbook of Photochemistry*; Marcel Dekker: New York, 1973).

(27) Xu, Z.; Eic, M.; Ruthven, D. In *Proceedings of the 9th International Zeolite Conference*, Montreal, 1992; von Ballmoos et al., Eds.; Butterworth-Heinemann: New York, 1993; pp 147-155.

(28) Turro, N. J. *Modern Molecular Photochemistry*; Benjamin/Cummings: Menlow Park, NJ, 1976; Chapters 9 and 14.

(29) Karger, J.; Ruthven, D. M. *Diffusion in Zeolites*; John Wiley & Sons: New York, 1992; Chapter 13.

(30) Atkins, P. W. *Physical Chemistry*; W. H. Freeman Company: New York, 1990; Chapter 25.

(31) (a) Garcia-Garibay, M.; Zhang, Z.; Turro, N. J. *J. Am. Chem. Soc.* 1991, 113, 6212. (b) Johnston, L. J.; Scavano, J. C.; Shi, J. L.; Siebrand, W.; Zerbetto, F. *J. Phys. Chem.* 1991, 95, 10018. (c) Yashonath, S.; Santikary, P. J. *Phys. Chem.* 1993, 97, 3849.

by filtration of the solvent was washed with dry hexane several times and dried under flowing nitrogen. Washing with hexane is believed to remove the aromatic molecules adsorbed on the outside surfaces of zeolites. Samples were taken in quartz ESR cells fitted with Teflon stopcocks and degassed thoroughly ( $10^{-5}$  mm). It was generally found that complete dehydration of the sample require degassing at elevated temperatures ( $\sim 100$  °C), and this was achieved by heating the sample while being on a vacuum line with a hot air gun for about 30 min. The absence of water was ensured by estimating the water content by thermogravimetric analysis and by monitoring the water uptake by using a Mettler balance. Emission spectral characteristics of the dry and wet samples significantly differed, and therefore, the extent of dryness was easily monitored by recording the emission spectra at room temperature.

**Coinclusion of Xenon and Oxygen.** Gaseous xenon (or oxygen) was coadsorbed onto the samples on a vacuum line. Samples dried as above were equilibrated with known pressures of xenon (or oxygen) for about 30 min, at which time a small drop in pressure was noticed, indicating the adsorption of gases onto zeolites. Gas pressure was monitored with an absolute-pressure transducer, MKS Baratron. Gas pressure, which could be controlled and monitored within  $\pm 0.1$  Torr, was varied between 5 and 760 Torr.

**Diffuse Reflectance Spectra.** Diffuse reflectance spectra of the zeolite solid samples were recorded in 2 mm path length quartz cells using a Varian 2400 spectrometer equipped with an integrating sphere (Varian); barium sulfate (Kodak, White Reflectance Standard) was used as the reference. Sample packing densities were not determined nor were they specifically controlled. Spectra were recorded between 220 and 800 nm. For comparison, spectra of the anhydrous zeolites were also recorded. Data were recorded digitally, and appropriate background corrections were carried out using the computer program, SpectraCalc (Galactic Industries).

**Emission Spectra.** Emission spectra were recorded at room temperature and at 77 K in Supracil quartz EPR tubes with a Spex Fluorolog 212 spectrofluorimeter. Emission intensity was monitored in a front face configuration. Spectra were corrected for detector sensitivity. Background scans of activated unloaded zeolite samples showed only a very weak emission in the 300–700-nm wavelength region, which did not interfere with the intense emissions from aromatics.

**Singlet Lifetime.** Fluorescence decays were monitored at room temperature and at 77 K in a front face configuration using an Edinburgh FL 900 single-photon counting apparatus. The decay was monitored for a duration of at least 7 lifetimes. Deconvolution was performed by nonlinear least squares routines minimizing  $\chi^2$  (software supplied with the instrument by Edinburgh), and goodness of fit was determined with plots of residuals, autocorrelation function, and reference to the Durbin-Watson statistic. The standard analysis algorithm used in this study allows curve fitting of up to four exponential terms, using the established Marquardt search method. None of our lifetime data could be analyzed as single-exponential decay. The total decay of all lifetime data (all points) could be fitted to two- and three-exponential decays with a reasonable  $\chi^2$  value. Noninclusion of the initial 15 ns on the analysis (two exponentials) generally gave excellent  $\chi^2$  values. The lifetimes for the two long components are essentially the same for both two and three exponentials, although the latter gave an additional short component ( $\sim 1$ –5 ns).

**Acknowledgment.** The author thanks D. R. Sanderson for excellent technical assistance and W. E. Farneth for useful discussion.